Multiplexed superconducting detectors for a neutrino mass experiment

Elena Ferri

University of Milano-Bicocca and INFN of Milano-Bicocca
on behalf of HOLMES collaboration

^{163}Ho Electron Capture for measuring the neutrino mass

$$^{163}\mathrm{Ho} + e^- \rightarrow \, ^{163}\mathrm{Dy}^* + \nu_e(E_c) \quad \text{electron capture from shell} \geqslant \mathrm{M1}$$

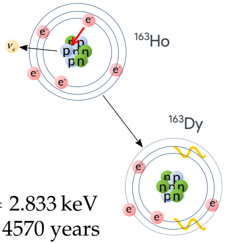

$Q_{EC} = 2.833\,\mathrm{keV}$
$\tau_{1/2} \simeq 4570$ years

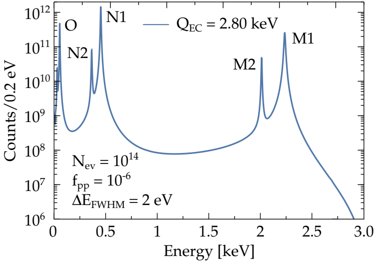

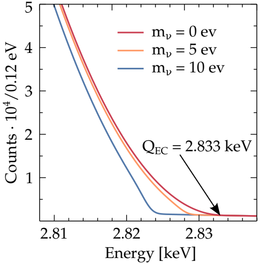

proposed for the first time
by A. De Rujula e M. Lusignoli in 1982
Phys. Lett. 118B (1982) 429
Nucl. Phys. B219 (1983) 277-301

- Calorimetric measurement of Dy atomic de-excitations (mostly non-radiative)

  $\Rightarrow$ measurement of the entire energy released except the ν energy

- rate at the end point depends on $(Q - E_{M1})$: the proximity to M1 resonance peak enhances the statistics at the end point (i.e. sensitivity on m_ν)

- Searching for a tiny deformation caused by a non-zero neutrino mass to the spectrum near its end point

^{163}Ho: pile-up spectra

$$S(E_c) = \left[N_{ev}(N_{EC}(E_c, m_\nu) + f_{pp} \times N_{EC}(E_c, 0) \otimes N_{EC}(E_c, 0)) + B(E_c)\right] \otimes R_{\Delta E}(E_c)$$

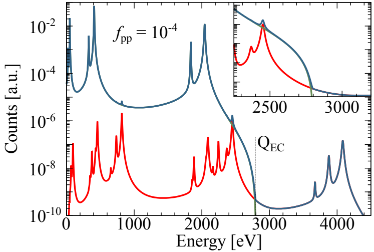

N_{ev}	: total number of events
$N_{EC}(E_c, m_\nu)$	: ^{163}Ho spectrum
$B(E)$	: background energy spectrum
$R_{\Delta E}(E_c)$	: detector energy response function
f_{pp}	: fraction of pile-up events
$R_{\Delta E}(E_c)$	: detector energy response function
ΔE	intervall of energy

more details on
Eur. Phys. J. C 74 (2014) 3161

- Pulse pile-up occurs when multiple events arrive within the temporal resolving time of the detector
- Unresolved pile-up events close to the end-point impairing effect on the end-point measurement
- The ^{163}Ho pile-up events spectrum is quite complex and presents a number of peaks at the end-point
- To resolve pile-up:
  - Detector with fast signal rise-time τ_{rise}
  - Pile-up recognition algorithm (i.e. Wiener filter, Singular Value Decomposition)

The m_ν statistical sensitivity has:

- **Strong** dependence on statistic: $\Sigma(m_\nu) \propto N_{events}^{1/4}$
- **Strong** dependence on pile-up: $f_{pp} \simeq A_{EC} \cdot \tau_{res}$
  (A_{EC}: pixel activity, τ_{res}: time resolution)
- **Weak** dependence on energy resolution ΔE;

Multiplaxable detectors with fast response are required

HOLMES

Neutrino mass determination with a sensitivity as low as ≈ 1 eV

- Microcalorimeters based on Transition Edge Sensors with ^{163}Ho implanted Au absorber
- Pixel activity of $A_{EC} \sim 300$ Bq/det
- Energy resolution: $O(\text{eV})$
- Time resolution: $\tau_{res} \sim 3\ \mu s$ ($\tau_{rise} = 10 - 20\ \mu s$);
- 1000 channels for $3 \cdot 10^{13}$ events collected in $T_M = 3$ years

more details on
Eur. Phys. J. C (2015) 75: 112

Pile-up Spectrum

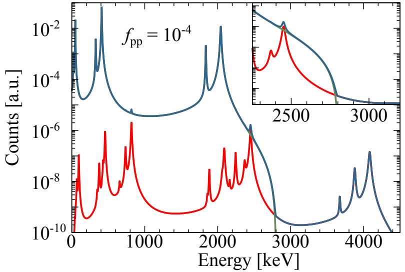

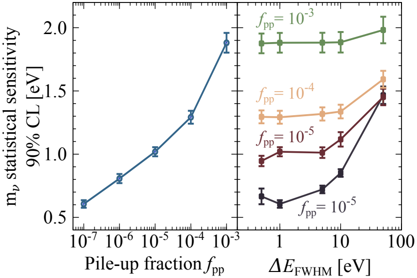

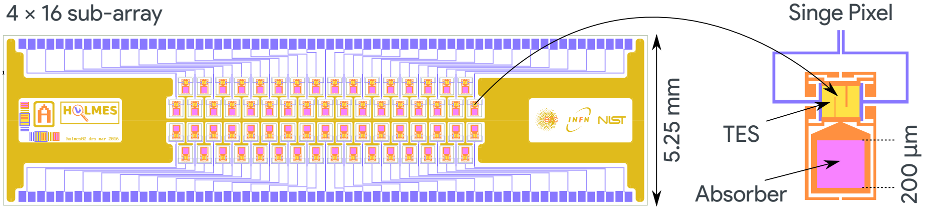

- Mo/Cu TES coupled to Gold absorbers where ^{163}Ho will be ion-implanted
- 2 µm Gold thickness for full e/γ absorption
- Side-car design to avoid TES proximitation effect
- Thermal conductance G engineering for τ_{decay} control
- 4 $\times$ 16 linear sub-array designed for high implant efficiency and low parasitic L
- Optimized design for high speed and high resolution:

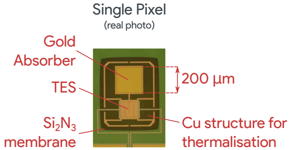

$$\text{Specs @ } 2.8\,\text{keV} : \Delta E_{FWHM} \simeq 3 - 4\,\text{eV}\,,\ \tau_{rise} \simeq 10\ \mu\text{s}\,,\ \tau_{decay} \simeq 100\ \mu\text{s}$$

^{163}Ho isotopes embedded in metallic absorbers (through ion-implantation)

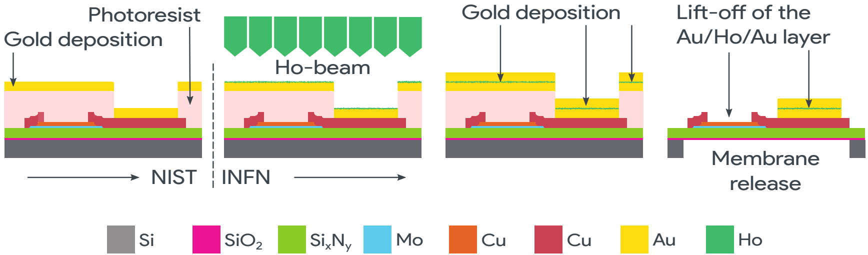

- Fabrication in two steps:
  - NIST: TES fabrication with 1 µm Au absorber
  - INFN: ^{163}Ho implantation, final deposition of 1 µm Au and SiN membrane release
- final micromachining step definition in progress

  ⇒ KOH vs DRIE machining

EUCAS 2021 SEPTEMBER, 5-9 MOSCOW

HOLMES TESs readout is based on microwave rf-SQUID multiplexing

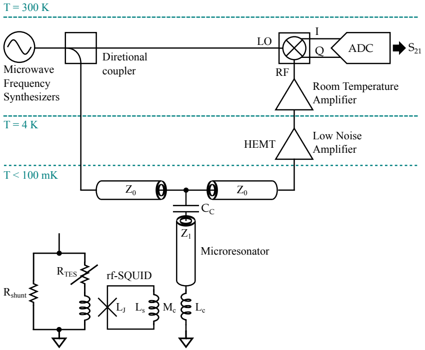

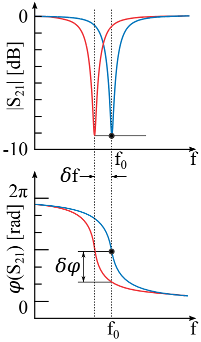

- rf-SQUID inductively coupled to a dc-biased TES and to a high-Q superconducting λ/4-wave resonator
- Change in TES current ⇒ change in the input flux to the SQUID
- The rf-SQUID transduces a change in input flux into a variation of resonant frequency and phase
- Each micro-resonator can be continuously monitored by a probe tone

EUCAS 2021 SEPTEMBER, 5-9 MOSCOW

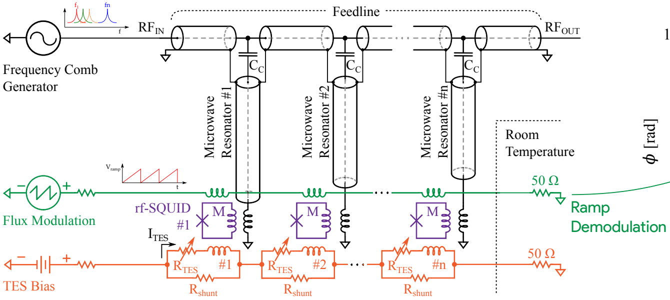

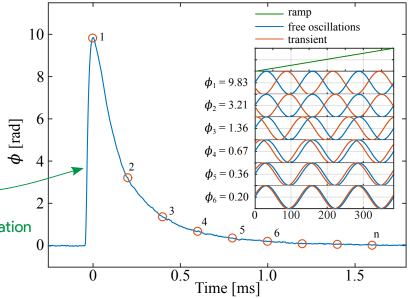

- By coupling many resonators to a single microwave feedline it is possible to readout multiple detectors
- Sensors are monitored by a set of sinusoidal probe tones (frequency comb)
- At equilibrium, the resonator frequencies are matched to the probe tone frequencies, and so each resonator acts as a short to ground
- The ramp induces a controlled flux variation in the rf-SQUID, which is crucial for linearizing the response
- Large multiplexing factor (> 100) and bandwidth, currently limited by the digitizer bandwidth

The Multiplexing chip

The core of the microwave multiplexing is the multiplexer chip

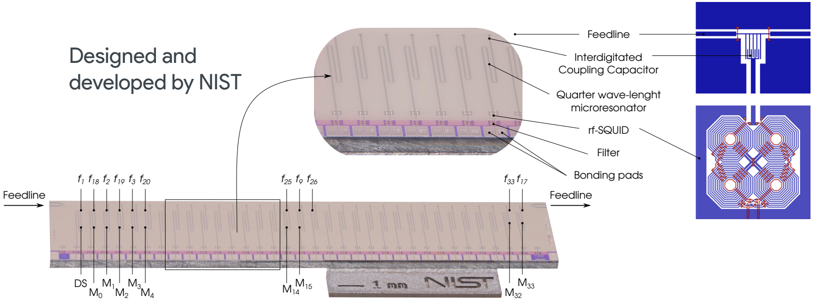

- Superconducting 33 quarter-wave coplanar waveguide (CPW) microwave resonators covering 500 MHz in the 4-8 GHz frequency range
- 200 nm thick Nb film deposited on high-resistivity silicon ($\rho > 10\,\mathrm{k}\Omega{\cdot}\mathrm{cm}$)
- each resonator has a trombone-like shape with slightly different length
- 2 MHz bandwidth per resonator
- separation beetween resonances 14 MHz (to prevent cross-talk)
- resonance depth greater than 10 dB
- squid equivalent noise less than $2\mu\phi_o/\sqrt{Hz}$

HOLMES DAQ with the ROACH2

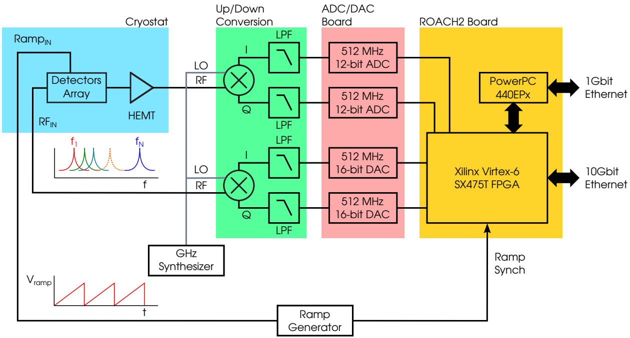

- Software Defined Radio with the open system ROACH2 (Casper collaboration)
- ADC BW 550 MHz
- real time pulse reconstruction

  → at the moment readout available for 64 channels

Multiplexing factor proportional to the target rise time

- $n_{TES} \approx 3.4 \cdot \tau_{rise}$
- requiring $\tau_{rise} = 10\mu s$

Multiplexing: characterization results

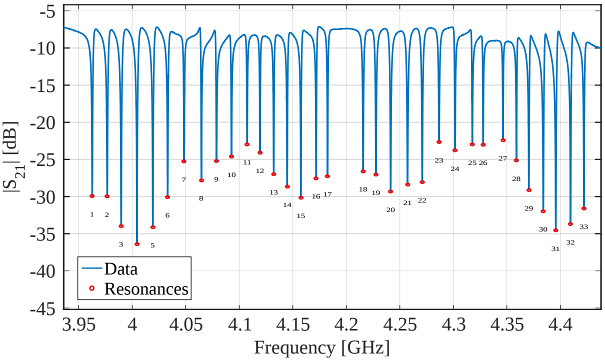

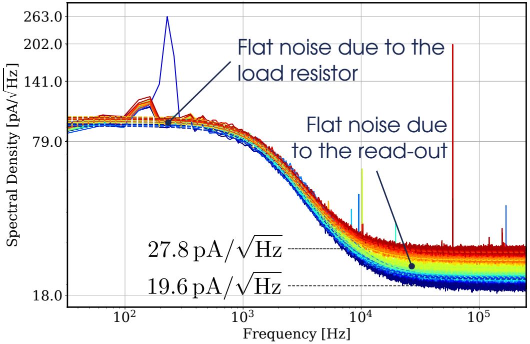

		Required	Measured
Resonators bandwidth	Δf_{BW} [MHz]	2	2 ± 1
Resonators spacing	Δf [MHz]	14	14 ± 1
Resonators depth	ΔS [dB]	> 10	29 ± 6

All the microresonator parameters match the HOLMES specification

Improved read out noise
$\rightarrow n_s = (23 \pm 2) pA/\sqrt{(Hz)}$
Previous work
$\rightarrow n_s = (26 \pm 7) pA/\sqrt{(Hz)}$

more details on
IEEE TAS 31 (2021) 5, 2100205

Multiplexing: characterization results (cont.)

Forward transmissiom S_{21} of 4 different band chips wired in series and an example of resonce fit

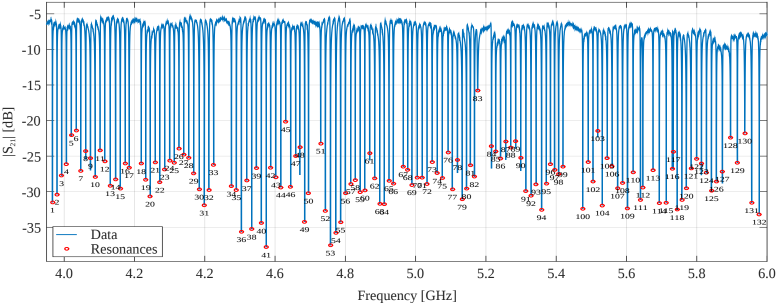

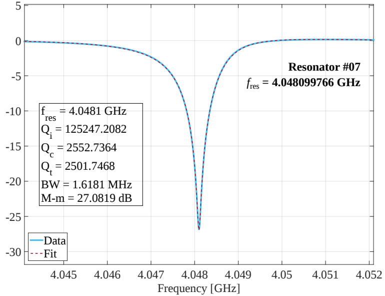

Four μmux in series are able to cover a wide frequency range from 4 to 6 GHz

HOLMES: test on the processed detectors

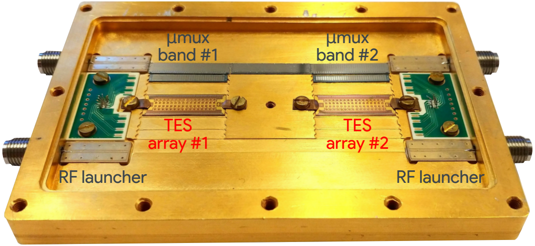

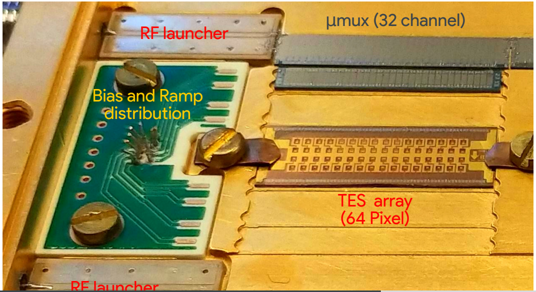

- Holder designed to host 128 Channels:
  - $2\times$ (4×16) sub arrays
  - $4\times$ μmux multiplexer chips with 4 bands
- 8 holders will cover the entire HOLMES in its final configuration (1024 channels);
- Preliminary low temperature tests performed with fully processed arrays (with KOH):
  - detector with (1 μm) absorber at NIST
  - absorber finalized (1 μm) at MIB
  - wet etching at MIB
- 32+32 TES pixels bonded (half of the available)
- Absorbers without the ^{163}Ho implanted
- New SDR firmwares for 16 and 32 channels:
  16-channel version fully operational
  32-channel version under testing
- New up/down-conversion system fully operational

HOLMES: detectors characterization with a fluorescence source

Event pulses due to the Manganese x-rays

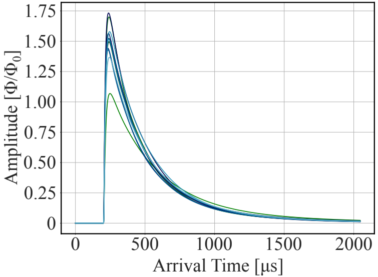

Uncalibrated energy spectra

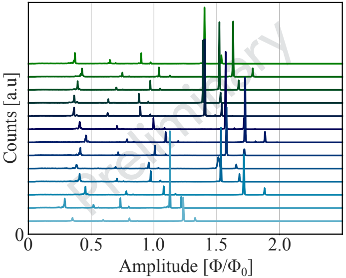

Noise Amplitude Spectral Density

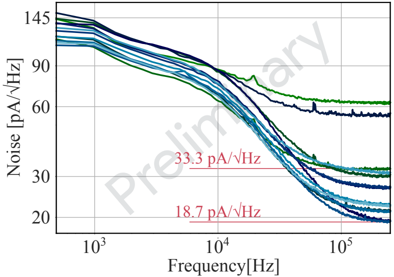

- non implanted detectors with KOH membrane release
- 13/16 working detectors (3 detectors with problematic resonators)
- Calibration run performed with a primary ^{55}Fe source faced to different targets
- X-ray fluorescence emission lines:

  ^{55}Mn (5.9 keV) ^{40}Ca (3.7 keV) ^{40}Cl (2.6 keV) ^{27}Al (1.5 keV)

Measured read out noise

$n_s \sim (19 - 33)\,\mathrm{pA}/\sqrt{\mathrm{Hz}}$

- Compatible with the previous prototypes
  Eur. Phys. J. C (2019) 79:304
- Two channels with higher noise due to not optimal rf-SQUID oscillations

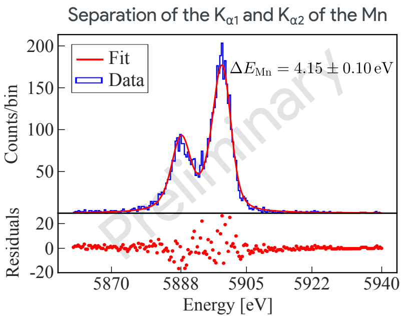

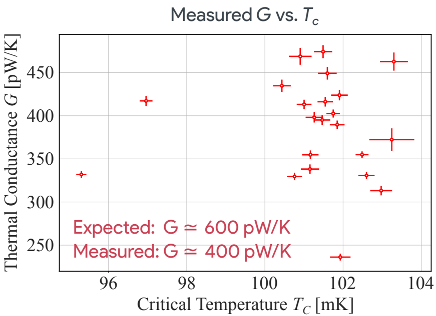

For the best detector: $\Delta E_{Mn} = 4.15 \pm 0.10$ eV @ 5.9 keV

- Energy resolution in the (4 - 6) eV range @ 5.9 keV

  Large spread probably due to the large G dispersion
  different G $\Rightarrow$ different working point
- $\tau_{rise} \simeq 20$ μs and $\tau_{fall} \simeq 300$ μs
  longer fall time due to lower thermal conductance G

KOH vs DRIE machining

- same energy resolution and rise time
- longer decay time and larger coupling dispersion